Palaeogeography, Palaeoclimatology, Palaeoecology 426 (2015) 216–228

Contents lists available at ScienceDirect

Palaeogeography, Palaeoclimatology, Palaeoecology

journal homepage: www.elsevier.com/locate/palaeo

Palynological evidence for prolonged cooling along the Tunisian continental shelf following the K–Pg boundary impact

Johan Vellekoop [a,*], Jan Smit [b], Bas van de Schootbrugge [a], Johan W.H. Weijers [c,1], Simone Galeotti [d], Jaap S. Sinninghe Damsté [c,e], Henk Brinkhuis [a,e]

[a] Marine Palynology and Paleoceanography, Laboratory of Palaeobotany and Palynology, Earth Science Department, Geosciences, Utrecht University, Budapestlaan 4, 3584 CD Utrecht, The Netherlands
[b] Eventstratigraphy, Department of Sedimentology and Marine Geology, VU University Amsterdam, de Boelelaan 1085, 1018HV Amsterdam, The Netherlands
[c] Geochemistry, Earth Science Department, Geosciences, Utrecht University, Budapestlaan 4, 3584 CD Utrecht, The Netherlands
[d] Department of Earth, Life and Environmental Sciences, University of Urbino 'Carlo Bo', Loc Crocicchia s.n., 61029 Urbino, Italy
[e] Royal Netherlands Institute for Sea Research (NIOZ), 1797 SZ 't Horntje, Texel, The Netherlands

ARTICLE INFO

Article history:
Received 29 October 2014
Received in revised form 3 March 2015
Accepted 11 March 2015
Available online 17 March 2015

Keywords:
Elles section
Cretaceous–Palaeogene boundary
Dinoflagellate cysts
Climate change
Sea level

ABSTRACT

The Cretaceous–Palaeogene (K–Pg) boundary mass extinction event is related to major global environmental changes resulting from a large extraterrestrial impact. Organic-walled cyst-producing marine dinoflagellates (dinocysts) survived the K–Pg mass-extinction relatively unscathed, making them ideally suited for reconstructing these environmental changes. So far, one of the best dinocyst records available is from the K–Pg boundary Global Stratotype Section and Point (GSSP) at El Kef (NW Tunisia). There, the dinocyst record shows major fluctuations across the boundary, likely reflecting strong responses to environmental changes. These fluctuations have so far not been confirmed by other studies. Therefore, in this study we performed a high-resolution marine palynological study on a closely spaced sample set from the Elles section, some 75 km south of El Kef, in order to generate a palaeoenvironmental and palaeoclimatic record across the K–Pg boundary to allow verification and refinement of earlier reported environmental changes. To better constrain the reconstructions based on qualitative biotic proxies we employed the quantitative sea surface temperature proxy TEX_{86}. Unfortunately, the TEX_{86} proxy record of the studied section is compromised because of post-depositional oxidation. However, the diverse dinocyst assemblages at Elles show strong fluctuations similar to the El Kef record, therefore confirming the earlier recorded signals, showing rapid, regionally consistent changes. These records imply that the latest Cretaceous was characterized by a gradual cooling trend and the onset of relative sea level fall. Within the immediate post-extinction interval, in the first thousands of years after the impact, dinocyst assemblages reveal multiple incursions of higher-latitude dinocyst species implying repeated pulses of cooling. These results signify that the earliest Danian climatic and environmental conditions were relatively unstable across the Tunisian shelf.

1. Introduction

The Cretaceous–Palaeogene (K–Pg) boundary (~65.5 Ma), is characterized by a major mass extinction event that has been widely attributed to the global environmental consequences of an impact of a large extraterrestrial body (Alvarez et al., 1980; Schulte et al., 2010). However, the precise killing mechanisms, and e.g., the distinct selectivity of the extinctions are still debated (e.g., D'Hondt, 2005) since there is much uncertainty about the precise climatic and ecological consequences of this impact. Numerical simulations of the global climatic effects of the K–Pg boundary impact predict a brief period of global cooling induced by sulphate aerosols blocking sun light — the so-called "impact winter" (Siggurdsson et al., 1992; Pope et al., 1997; Pierazzo et al., 2003), followed by a period of greenhouse warming caused by CO_2 released into the atmosphere by the impact (Kring, 2007). These major environmental perturbations likely played a major contributory role in the K–Pg boundary mass extinction (Vellekoop et al., 2014). Unfortunately, it has proven difficult to confirm these models, as major extinctions amongst traditional proxy-carriers, e.g., planktic foraminifera, hamper accurate palaeoenvironmental reconstructions (Hull et al., 2011). Consequently, studies of sufficient detail to elucidate the possible global environmental consequences of the impact and related mechanisms, or to test various aftermath scenarios, are generally lacking (Kring, 2007).

One biotic proxy-record that holds great promise to shed light on the environmental conditions governing the ocean–climate system pre- and post-impact are organic-walled dinoflagellate cysts (dinocysts).

* Corresponding author at: Division Geology, Department of Earth and Environmental Sciences, KU Leuven University, Celestijnenlaan 200E, 3001 Leuven, Belgium. Tel.: +32 16 37 77 80.
E-mail address: johan.vellekoop@ees.kuleuven.be (J. Vellekoop).
[1] Present address: Royal Dutch Shell, 2288 GS, Rijswijk, The Netherlands.

http://dx.doi.org/10.1016/j.palaeo.2015.03.021
0031-0182/

Dinocysts can be used to reconstruct a wide range of environmental parameters, including temperature, salinity, and nutrients. Moreover, this group does not show accelerated rates of extinction across the K–Pg boundary (Brinkhuis and Leereveld, 1988; Brinkhuis and Zachariasse, 1988; Brinkhuis et al., 1998), making them ideally suited to qualitatively assess latest Maastrichtian to earliest Danian changes in palaeoenvironment, palaeoceanography and palaeoclimate. In addition, dinocysts do provide the highest possible biochronostratigraphic resolution across this interval (Habib et al., 1996; Brinkhuis et al., 1998; Açikalin et al., 2015).

Amongst the best sites to unravel these changes are the stratigraphically complete and expanded sections of the El Haria Formation in Tunisia, including the Global Boundary Stratotype Section and Point (GSSP) of the Danian Stage at El Kef (Molina et al, 2006). The El Kef section has already provided one of the most complete, stratigraphically expanded and well-preserved dinocyst records across the K–Pg boundary (Brinkhuis and Leereveld, 1988; Brinkhuis and Zachariasse, 1988; Brinkhuis et al., 1998). Interestingly, in contrast to model predictions, the dinocyst distribution patterns and benthic foraminifera at El Kef suggest multiple cooling pulses in the earliest Palaeocene (Brinkhuis et al., 1998; Galeotti et al., 2004). These climatic perturbations likely contributed to the biotic stress at the K–Pg boundary. Yet, these fluctuations have so far not been confirmed by other studies and it is unknown how and if they might be related to environmental changes independent of the impact event, such as background climate and sea-level fluctuations.

The expanded Elles I section, approximately 75 km south of El Kef, also comprises a complete K–Pg boundary succession and is presumed to be deposited in a more proximal shelfal setting (e.g., Adatte et al., 2002). This section provides an opportunity to corroborate the signals earlier recorded at El Kef. We therefore performed a high-resolution marine palynological study on a closely spaced sample set from the Elles section, in order to generate a palaeoenvironmental and palaeoclimatic record across the K–Pg boundary to allow verification of earlier reported environmental changes from the nearby El Kef. In order to better constrain the reconstructions based on biotic environmental proxies we employ the biomarker-based sea surface temperature proxy TEX_{86} (Schouten et al., 2002).

2. Geological setting

This study focuses on the K–Pg boundary interval of the El Haria Formation in north-western Tunisia. This formation encompasses some of the most complete K–Pg boundary transitions currently known, including the K–Pg boundary GSSP at El Kef and the Elles I section, investigated in the current study. Today these sites are located at 35–36°N, but at Cretaceous–Palaeogene times, their position was in the arid climate zone in the low latitudes, near the tropic of Cancer (around 20–25°; Scotese, 2004). The Elles and El Kef sections are palaeogeographically situated in the Tethys Ocean, on the African continental shelf (Fig. 1).

The Elles section shares many similarities with the K–Pg stratotype section at El Kef. It is located near the small settlement of Elles, 75 km from El Kef, in the Karma Valley (35°56′43.73″N, 9°4′48.15″E), Tunisian Central Atlas (Karoui-Yaakoub et al., 2002). The K–Pg boundary transition is exposed at two tributaries of the Karma Valley. The exposures in the right valley fork have been called the Elles I section and the exposures in the left valley fork have been called the Elles II section (Adatte et al., 2002). In this study, we focus on the Elles I section since it is best documented (Adatte et al., 2002). It mainly consists of marly and clayey sediments ($CaCO_3$ content between 30% and 60%). Similar to El Kef, the sequence is interrupted at the K–Pg boundary by a dark, ~50 cm thick, carbonate depleted (<10%) interval, the boundary clay layer (Adatte et al., 2002; Coccioni and Marsili, 2007). The K–Pg boundary is located at the base of the boundary clay layer, where a 3–4 mm-thick rusty red (Fe-oxide rich) layer occurs. The boundary clay layer contains global K–Pg boundary markers such as an anomalous concentration in Ir, Ni-rich spinels, and altered microtektites (e.g., Coccioni and Marsili, 2007).

The Elles sections are interpreted to be deposited in middle to outer shelf depths (at an estimated palaeo-water depth of about ~150 m; Adatte et al., 2002), a slightly more proximal position than the El Kef section, resulting in a generally higher terrigenous influx and hence a sedimentation rate exceeding that of the El Kef section (Abramovich and Keller, 2002; Adatte et al., 2002; Stüben et al., 2002). Various authors have suggested that Maastrichtian sedimentation rates at Elles were about 3–4 cm/kyr (e.g., Adatte et al., 2002; Stüben et al., 2003) and Danian sedimentation rates have been estimated to be between 2–4 cm/kyr (Galeotti et al, 2005).

Since the Elles section comprises a complete and expanded K–Pg boundary interval with a better exposure of the boundary than the K–Pg GSSP at El Kef, it has been proposed as parastratotype (e.g., Karoui-Yaakoub et al., 2002) and has been studied in great detail in the last decades, presenting an ideal section to verify the signals recorded at El Kef.

3. Biostratigraphy

The El Kef K–Pg boundary GSSP is one of the best studied K–Pg boundary sections in the world and has a detailed planktic foraminifera, calcareous nannofossil and dinocyst biostratigraphy (Molina et al.,

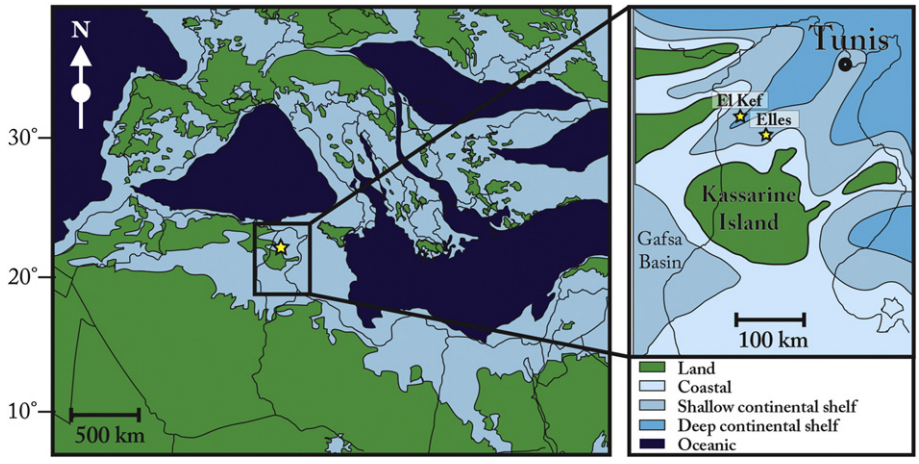

Fig. 1. Late Cretaceous–Palaeogene palaeogeography of the Mediterranean region and a detailed palaeogeographic setting of Tunisia, with the location of the Elles and El Kef sections. Palaeogeographical reconstruction based on Scotese (2004) and Scotese and Dreher (2012).

2006) allowing a precise zonation of the boundary interval. The biostratigraphic framework for the Elles section is less detailed. Planktic foraminiferal biostratigraphy allows the most detailed zonation of the studied interval, which extends from 5 m below to 4 m above the K–Pg boundary interval, covering the uppermost Maastrichtian and lowermost Danian (Karoui-Yaakoub et al., 2002; Coccioni and Marsili, 2007). The biostratigraphic records of the Elles section indicate that the K–Pg boundary is stratigraphically complete at this section. For more information on the biostratigraphy of the Elles section, see Supplementary Materials 1.

To allow the most precise biostratigraphic dating of inferred changes and enable accurate comparison, we apply a foraminiferal zonation similar to that used in Brinkhuis et al. (1998), which closely resembles that of Smit and Romein (1985) and Vellekoop et al. (2014) (see Fig. 2). Given that the zonal marker *Parvulorugoglobigerina minutula* was not recorded in Elles, the P0/P1a zonal boundary of Smit and Romein (1985) cannot be exactly identified. However, since the First Appearance Datum (FAD) of *P. minutula* is just before the FAD *Parvulorugoglobigerina fringa*, the P0/P1a zonal boundary of Smit and Romein (1985) must be very close to the First Occurance (FO) of *P. fringa*, permitting a tentative placement of this zonal boundary in the Elles section, just below the FO of *P. fringa*.

4. Methods

4.1. Sampling

To develop a high-resolution dinocyst record across the K–Pg boundary, closely spaced samples were obtained from the Elles section. A total of 100 samples have been collected at 5-cm spaced intervals from the uppermost five metres of the Maastrichtian. We use splits from ten 50-cm-long continuous sections that have been obtained from the lowermost Danian part of the Elles section to form a composite core of 411 cm when depth is corrected by dip within individual sections. These sections have been obtained by using a metal box hammered into a deeply dug trench (for a description of the sampling procedure, see Galeotti et al., 2005).

4.2. Palynological processing

In total, 236 samples from the Elles section were processed following standard palynological processing techniques. Briefly, approximately 4 g of each sample was crushed, oven dried (60 °C) and weighted, and a known amount (10,679, error 5%) of *Lycopodium clavatum* spores was added. The samples were then treated with 10% HCl and 40% HF to dissolve carbonate and silicate minerals, respectively. No heavy liquid separation or oxidation was employed. After each acid step, samples were washed with water and centrifuged or settled for 24 h and decanted. The residue was sieved over nylon mesh sieves of 250 μm and 10 μm and treated with ultrasound for 5 min to break up agglutinated particles of the residue. From the residue of the 10–250 μm fraction, quantitative slides are made on well mixed, representative fractions by mounting one droplet of homogenised residue and adding glycerine jelly. The mixture was homogenised and sealed. All slides are stored in the collection of the Laboratory of Palaeobotany and Palynology, Utrecht University.

For the present study, of ~60 of these samples (20 samples from the Maastrichtian interval and ~40 samples from the Danian interval), the palynomorphs were counted up to a minimum of 200 dinocysts. The taxonomy of dinocysts follows that cited in Fensome and Williams (2004). A species list can be found in Supplementary Materials 2.

4.3. Organic-walled dinoflagellate cysts

Dinocysts provide a powerful biostratigraphic tool and various high-resolution studies have been performed across the K–Pg boundary (e.g., Moskovitz and Habib, 1993; Brinkhuis and Schiøler, 1996; Brinkhuis et al., 1998). In addition, they provide means to reconstruct changes in palaeoproductivity and several other environmental parameters such as coastal proximity, sea surface temperature (SST) and salinity (SSS) using inferred ecological affinities (e.g., Sluijs et al., 2005). Brinkhuis and Biffi (1993) have argued that the relative contribution of high/middle-latitude (cool-temperate) taxa vs. low-latitude/Tethyan (warm) taxa can be used to reconstruct SST trends in the Palaeogene. This method has also been applied to infer palaeo-temperature trends

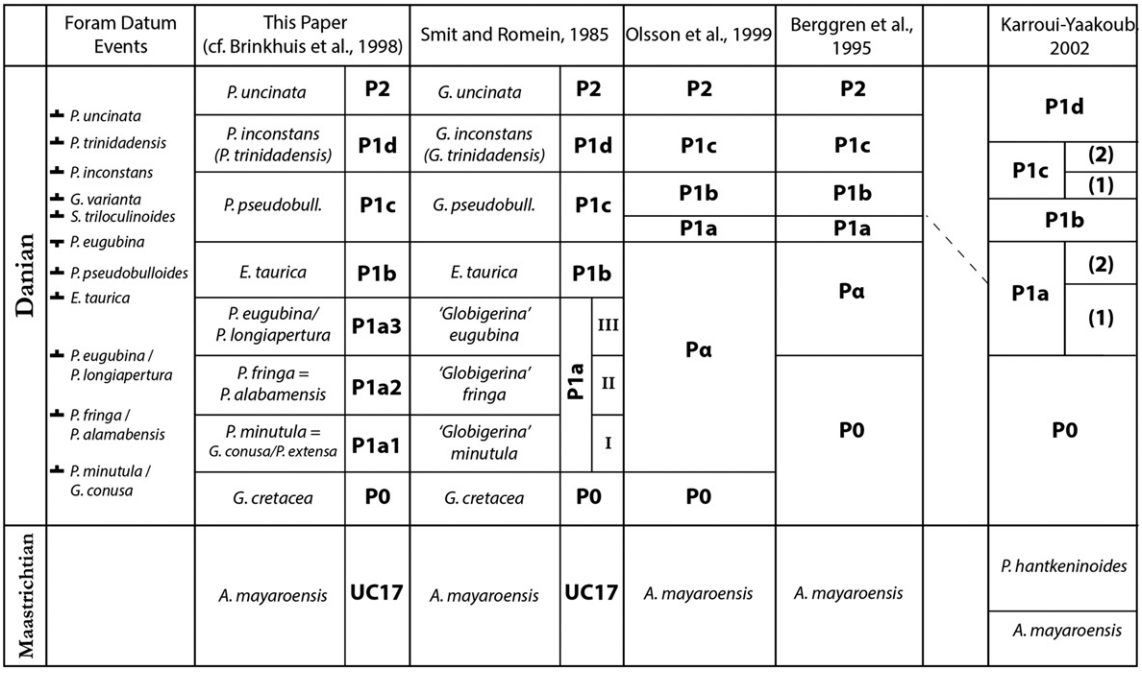

Fig. 2. Planktic foraminiferal biostratigraphic zonation of the K–Pg boundary interval. First and Last Appearance Datums of important index species are indicated. The zonation applied here is similar to that used in Brinkhuis et al. (1998) and is here compared to the zonations of Smit and Romein (1985), Olsson et al. (1999), Berggren et al. (1995) and Karoui-Yaakoub et al. (2002).

across the K–Pg boundary interval (Brinkhuis et al., 1998). In the latter study, a combination of two methods was used. First, apparent latitudinal preferences of taxa were identified by means of a literature study. Brinkhuis et al. (1998) argue that, in the Tunisian record, taxa like *Palynodinium grallator* and *Achilleodinium biannii* represent typical high-latitude influences, whereas for example *Senegalinium bicavatum* appears to be a low latitude taxon. However, although dinocysts have been demonstrated to be a useful tool in reconstructing the palaeoenvironment (e.g., Brinkhuis et al., 1998; Sluijs et al., 2005), the still relatively poor knowledge of ecological preferences of many, extinct species often hampers more detailed environmental reconstructions. In general, it may be helpful to use statistical methods such as Detrended Correspondence Analysis (DCA; Hill and Gauch, 1980) for this purpose. Versteegh and Zonneveld (1994) have shown that DCA is a useful tool to determine the ecological preferences of extinct dinoflagellate cyst species. Therefore, Brinkhuis et al. (1998) also used Detrended Correspondence Analysis (DCA) to identify temperature relationships within the dataset.

To allow a good comparison between the Elles and El Kef records, an approach similar to Brinkhuis et al. (1998) was used in the present study. To be able to accurately compare the dinocyst record of the present study with that of El Kef, the microscope slides used by Brinkhuis et al. (1998), stored at the Laboratory of Palaeobotany and Palynology in Utrecht, Utrecht University, were re-examined to standardize the taxonomy used in these studies. For this taxonomic standardization, single-grain preparations of type-specimens of Brinkhuis et al. (1998) were also examined.

In order to recognize the main environmental trends, DCA was carried out on a selected part of the data using PAST (Hammer et al., 2001), following procedures described in Brinkhuis et al. (1998). The species selected for this analysis are discussed in Supplementary Materials 4.

4.4. TEX_{86} analyses

In an attempt to quantify the SST changes recorded by the dinocyst record, 40 aliquot samples were investigated for TEX_{86} palaeothermometry following standard procedures (Schouten et al., 2002, 2013). Briefly, organic compounds were extracted from powdered and freeze-dried rock samples of approximately 5 g with dichloromethane (DCM)/methanol (MeOH) (9:1, v/v) using a DIONEX accelerated solvent extractor (ASE 200). The total extracts were separated in 4 fractions over an activated Al_2O_3 column successively using hexane:dichloromethane (DCM) (9:1, v/v), ethyl acetate (100%), DCM:MeOH (95:5, v/v) and DCM:MeOH (1:1, v/v). Following this, 250 ng of a C_{46} Glycerol Trialkyl Glycerol Tetraether internal standard (Huguet et al., 2006) was added to the DCM:MeOH (95:5, v/v) fraction for quantification purposes. Samples were analysed using high performance liquid chromatography/atmospheric pressure positive ion chemical ionization mass spectrometry (HPLC/ APCI-MS) according to Schouten et al. (2007). For a more detailed description of this technique and its application, see Schouten et al. (2002, 2007, 2013). The TEX_{86} index values were calculated following Schouten et al. (2002).

5. Results

5.1. TEX_{86}

Most of the samples analysed for TEX_{86} contained traces of crenarchaeotal GDGT lipids, but their overall concentrations were only just above detection limit. Unfortunately, poor signal to noise ratios make temperature reconstructions based on these biomarkers less reliable. A further complication was that the sediments are characterized by relatively high BIT-index values (0.06–0.78) (see Table 1) The BIT-index is a proxy indicative for the input of soil-organic matter. Since sediments with high input of soil organic matter also receive a contribution of terrestrial isoprenoid GDGTs, they may yield relatively unreliable SST estimates (Weijers et al., 2006). Therefore, also the high BIT-index values prevent to generate an accurate temperature record across the K–Pg boundary. The generally high BIT-index values are rather surprising given the relative offshore setting and the minor contribution of terrestrial components to the palynomorph assemblages. Perhaps these high BIT index values resulted from contamination by modern rather than representing original fossil soil organic matter. Alternatively, since marine GDGTs are relatively more labile than terrestrial GDGT (Lengger et al., 2013), the relatively high BIT-index values and the large variation throughout the record might be the result of post-depositional oxidation. Consequently, the resulting TEX_{86} and BIT-index records are relatively chaotic and probably unreliable.

Table 1
Table with samples processed for GDGT analyses. Per sample, where available, the yield (in ng/g total GDGTs) and BIT-index are indicated. Samples with BIT-index above the recommended threshold of 0.3 (Weijers et al., 2006) are indicated in grey. Note the variable nature of the BIT-index record.

Sample	Distance from K–Pg boundary (cm)	Yield (ng/g)	BIT–index
ELLES 10	405	n.a.	0.74
ELLES 9–34/35/36	373	n.a.	0.24
ELLES 8–2/3/4	302	0.6	0.38
ELLES 6–4/5	229	n.a.	0.42
ELLES 6–1/2/3	226	n.a.	0.41
ELLES 5–34	220	2.4	0.27
ELLES 4–18/19	146	1.1	0.23
ELLES 3–18	97	0.5	0.34
ELLES 2–38	66	1.9	0.56
ELLES 2–22	49	0.9	0.32
ELLES 2–16	43	1.1	0.43
ELLES 2–10/11	36	n.a.	0.26
ELLES 2–5/6	31	0.4	0.18
ELLES 1–21	23	1.7	0.30
EL T7	20	n.a.	0.78
ELLES 1–18/19	18	0.6	0.27
ELLES 1–13/14	13	1.2	0.17
ELLES 1–9	9	2.3	0.26
ELLES 1–5	5	1.2	0.16
ELLES 1–4	4	0.9	0.27
EL T2	1	n.a.	0.62
ELLES 1–1	1	2.1	0.29
EL IL	0	37.6	0.41
EL T	−1	0.6	0.06
EL −2	−2	n.a.	0.08
EL 2	−8	n.a.	0.15
EL 6	−28	2.5	0.12
EL 9–10	−48	0.5	0.08
EL 13	−63	n.a.	n.a.
EL 14/15	−70	1.9	0.30
EL 31	−153	0.6	0.17
EL 43/44	−215	n.a.	0.24
EL 48	−238	16.9	0.42
EL 62	−308	0.8	0.19
EL 72	−358	n.a.	0.14
EL 82/83	−410	n.a.	0.29
EL 88/89	−440	1.5	0.30
EL 92/93	−460	1.5	0.55
EL 96–100	−480	n.a.	0.69

5.2. Elles section palynology

In general, the Elles section comprises rich, well to excellently preserved palynomorph assemblages. All samples yielded palynological assemblages very similar to those at El Kef. Hence, the results from the Elles section can be used to verify the earlier reported signals at the El Kef section. The Elles section record is dominated by marine palynomorphs (75–90% of the assemblage), with a dominance of the representatives of the genus *Spiniferites*, and the morphologically related genus *Achomosphaera*, and an overall relative high abundance of

peridinioid dinocysts. Other categories of palynomorphs that were encountered include different types of acritarchs, foraminiferal linings, bisaccate pollen, angiosperm pollen, trilete spores and different genera of fresh- to brackish water algae (predominantly *Paralecaniella indentata*, *Botryococcus* sp. and *Tasmanites* sp.).

5.3. Elles biostratigraphy

The dinocyst record comprises several first and last occurrences of biostratigraphically important species (referred to as 'dinocyst events'). These include the FAD and Last Appearance Datum (LAD) of *P. grallator* and the FADs of *Senoniasphaera inornata*, *Damassadinium californicum*, *Carpatella cornuta* and *Laternosphaeridium reinhardtii*, which permit a detailed zonation of the most basal part of the Danian (Brinkhuis et al., 1998) (see Fig. 3). The interval above this can be stratigraphically correlated using the FOs of the planktic foraminiferal species *Parvulorugoglobigerina longiapertura*, *P. fringa* and *Parvulorugoglobigerina eugubina*. The resulting biostratigraphic correlation between the Elles and El Kef sections is shown in Fig. 4.

In the past, the typical Late Cretaceous group *Dinogymnium* spp. and the morphologically related *Alisogymnium* spp. have been considered the single group of organic-walled cyst producing dinoflagellate species to go extinct at the K–Pg boundary (Williams et al., 2004). At both Tunisian records, this group has rare occurrences in the late Maastrichtian, but also throughout the lower half of the Danian interval. This might be related to reworking, but, alternatively, since this phenomenon has also been recorded at various other K–Pg boundary sites (e.g., Brazos River, Braggs, Geulhemmerberg) (e.g., Brinkhuis and Schiøler, 1996; Vellekoop et al., 2014), the LAD of *Dinogymnium* spp. and *Alisogymnium* spp. may actually be slightly younger, occurring in the early Danian rather than precisely at the K–Pg boundary.

5.4. Elles section palaeoecology

While dinocysts are the dominant palynomorphs throughout the studied interval, terrestrial elements and fresh- to brackish water algae show a small increase in abundance across the K–Pg boundary at the Elles section, reaching maximum values about 80–100 cm above the boundary. The ratio of terrestrial over marine palynomorphs (t/m) stays between 0 and 0.04 in the Maastrichtian and increases up to 0.11 in the lowermost Danian, to return to ~0.08 at the top of the studied interval. The relative distribution of the recorded categories of palynomorphs and the t/m ratio of the studied samples are plotted in Fig. 5.

The studied interval is characterized by diverse dinoflagellate cyst assemblages. In total, some 120 different dinocyst taxa were identified. An alphabetical species list of dinocyst taxa is provided in Supplementary Materials 2. The most abundant dinocyst group in the record is the *Spiniferites ramosus* complex and the morphologically related genus *Achomosphaera* (~5–45% of the assemblage). Other abundant species are *Glaphyrocysta perforata*, *S. bicavatum* and *Pierceites pentagona*, all of which generally account for 1–25% of the assemblage. In the lower part of the studied interval the typically outer neritic and normal marine dinocyst taxa, such as the *Spiniferites* group, are dominant and open marine, oceanic dinocyst taxa, such as the *Impagidinium* spp. and *Pyxidinopsis* spp. (cf. Sluijs et al., 2005) are also relatively abundant. Members of the *Areoligera*/*Glaphyrocysta* group are most abundant above the K–Pg boundary.

Presumed heterotrophic peridinioid dinoflagellates (Sluijs et al., 2005) are very abundant in the Elles record (up to 80% of the assemblage). The P/G ratio, here defined as the ratio of peridinioid dinocyst specimens over gonyaulacoid dinocyst specimens, sensu Versteegh (1994), varies between 0.22 and 0.79 during the Maastrichtian (with an average of 0.43), decreases sharply to 0.13 at the K–Pg boundary and subsequently increases to values similar those for the Maastrichtian (see Fig. 5). Strikingly similar to the El Kef record, at Elles the presumably opportunistic, heterotrophic group composed of the tropical genera *Andalusiella* and *Palaeocystodinium* (referred to as the 'A–P complex'; Brinkhuis et al., 1998) rapidly increases in abundance approximately 10 cm above the boundary, peaking at 19 cm above the K–Pg boundary, in the upper part of Zone P0 (Brinkhuis et al., 1998; this study). At this peak, the A–P complex makes up ~38% of the assemblage. The peak of the A–P complex results from an increase in absolute abundances, up to 2500 cysts per gramme (see Fig. 6). Once the A–P complex abundance decreases again, other peridinioid cysts once more become dominant and restore to pre-K–Pg boundary concentrations.

The assemblage is generally dominated by groups that are regarded either as cosmopolitan or to have low latitude affinities by Brinkhuis et al. (1998), such as the *S. ramosus* complex, *Pierceites pentagonia* and *S. bicavatum*. Crucially, similar to the El Kef section, at Elles the basalmost Danian is characterized by the influx of higher-latitude taxa, most notably with the FOs of *P. grallator* and *Palaeoperidinium pyrophorum* and the increase in abundance of inferred higher-latitude species such as *Cribroperidinium* sp. A of Brinkhuis and Schiøler (1996) and *A. biannii*.

5.5. Statistical analysis

In order to recognize the main environmental trends such as temperature relationships within the dataset, a DCA was carried out on a selected part of the data, approximately following procedures described in Brinkhuis et al. (1998). For the DCA presented in this study, all species with less than 15 specimens in the total dataset of 20,000 were omitted. A more detailed explanation of the criteria used can be found in Supplementary Materials 3. The distribution of the selected taxa along the two most important DCA-axes is plotted in Fig. 7. In the distribution of the taxa along the first axis (eigenvalue 0.175) two main clusters can be recognized, with several outliers on the right side of the graph. The main cluster on the left-hand side of the plot includes inferred low-latitude species such as *P. pentagonia*, *S. bicavatum* and the *Fibrocysta*/*Kenlyia* group. Inferred cosmopolitan taxa, such as *Spiniferites*/*Achomosphaera* spp. and *Florentinia mantellii*, plot in the central cluster. The outliers on the right-hand side represent typical species included in the group of higher-latitude taxa of Brinkhuis et al. (1998), such as *Cribroperidinium* sp. A of Brinkhuis and Schiøler (1996), *A. biannii* and *Glaphyrocysta pastielsii*. This suggests that the first DCA-axis can be interpreted as a sea surface temperature gradient. The loadings on DCA-axis 1 through the studied interval are plotted in Fig. 8.

A division criterion as indicated in Fig. 7 can be used to split the dinocyst assemblage into groups, in a similar manner as Brinkhuis et al. (1998). The combined percentage of the "higher-latitude" group that is created this way provides an indication of the contribution of higher-latitude species to the total assemblage. The loading on DCA-axis 1 and the combined percentage of the cold water species group are two different ways to qualitatively reconstruct sea surface temperature changes across the studied interval, with the first portraying the trend in the data and the latter showing the intervals that SST likely was low enough for a significant ingression of "Boreal" taxa (see Fig. 8).

The assemblage appears to have a normal distribution along the second axis of the DCA (eigenvalue of 0.121), with most taxa clustering in the middle. Most peridinioid cysts plot in the upper half of the graph, including typical peridinioid genera with hexagonal archeopyles such as *Senegalinium* and *Cerodinium*, which have been suggested to be indicative for freshwater input (Sluijs and Brinkhuis, 2009). This implies that the second axis of the DCA might correspond to nutrient and/or freshwater input. The fact that much of the inferred neritic gonyaulacoid genera, such as *Areoligera*, *Glaphyrocysta* and *Operculodinium* are also positioned in the upper half of the plot, whereas more oceanic genera such as *Impagidinium*, *Spiniferites* and *Pyxidinopsis* plot in the lower half of the plot suggest that this axis presents an indication of coastal proximity, characterized by gradients in nutrient and/or salinity.

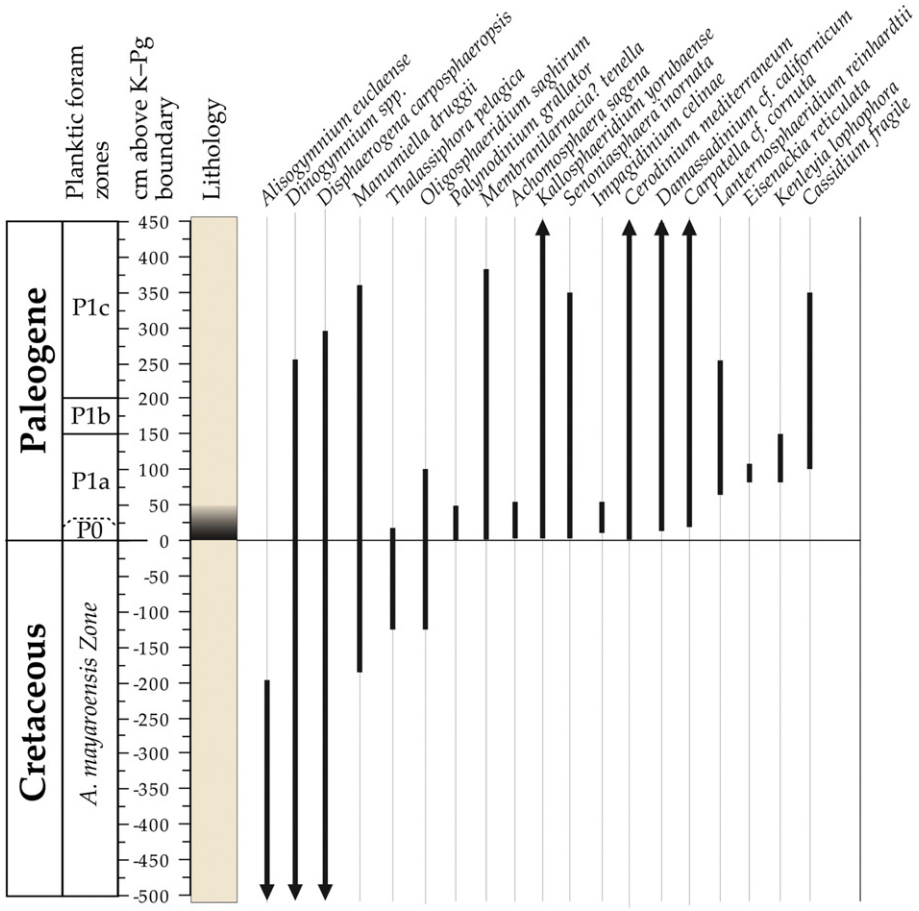

Fig. 3. Stratigraphic ranges of selected dinoflagellate cyst taxa at the Elles section. Taxa included are considered important stratigraphic index species for the K–Pg boundary in previous studies (e.g., Moskovitz and Habib, 1993; Brinkhuis et al., 1998; Williams et al., 2004; Slimani et al., 2010) and have a Last Appearance Datum or First Appearance Datum within the studied interval.

Therefore, the loadings of DCA-axis 2 and the palynological assemblages can be used to reconstruct relative sea level changes across the studied interval (Fig. 9).

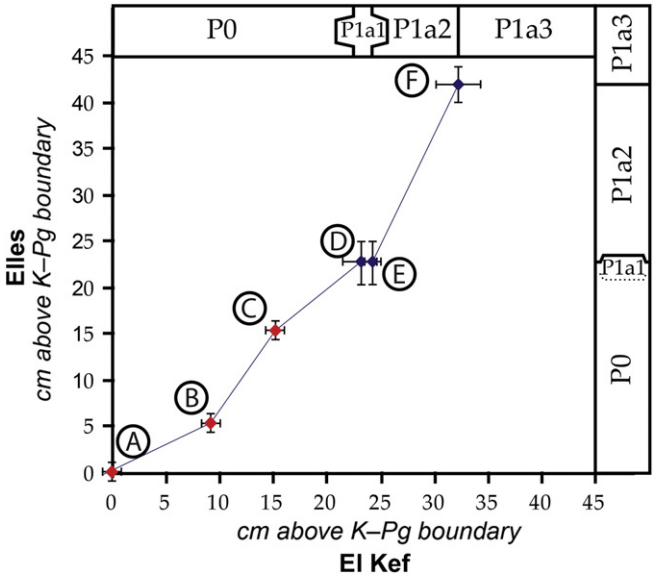

Fig. 4. A correlation of the lowermost Danian biostratigraphic events in the El Kef and Elles sections. A) FO *P. grallator*; B) FO *S.* cf. *inornata*; C) FO *D.* cf. *californicum*; D) FO *P. minutula*; E) FO *P. fringa*; F) FO *P. eugubina*. The exact depths of the biostratigraphic events are indicated in Supplementary Materials 3.

Interestingly, *Manumiella druggii* and the A–P complex, both peridinioid taxa, plot in the lower part of the DCA, amongst more offshore taxa. Some authors have suggested that *M. druggii* is indicative for shallow marine conditions, potentially even in low salinity environments (e.g., Hultberg and Malmgren, 1987), contradicting our interpretation of DCA-axis 2. Conversely, our results suggest that this presumably heterotrophic species can also occur in more open ocean conditions. Conspicuously, both *M. druggii* and the A–P complex show blooms in our record. These peak occurrences likely resulted from other environmental or ecological changes and are therefore probably not controlled by coastal proximity.

5.6. Comparison between the Elles and El Kef sections

The palynological record of the Elles is very similar to that of El Kef, both biostratigraphically as well as in terms of species composition. The interval calibrated against Zones P0 and P1a1 is of similar thickness in both sections, whereas the interval calibrated against zones P1a2, P1a3, P1b and P1c is slightly more expanded at the Elles section (see Fig. 4). The higher sedimentation rates at Elles, which have previously been related to the more proximal setting of this site (Adatte et al., 2002), are thus confirmed. The only major stratigraphical discrepancy between El Kef and Elles is the LO of *P. grallator*. At El Kef, this taxon has its LO at 25 cm above the boundary, whereas at Elles *P. grallator* appears to have a slightly longer range, as it occurs up to 50 cm above the boundary. Planktic foraminifera and dinocyst biostratigraphy show that together, the El Haria K–Pg boundary sites can be regarded as the most expanded complete K–Pg boundary sites in the world.

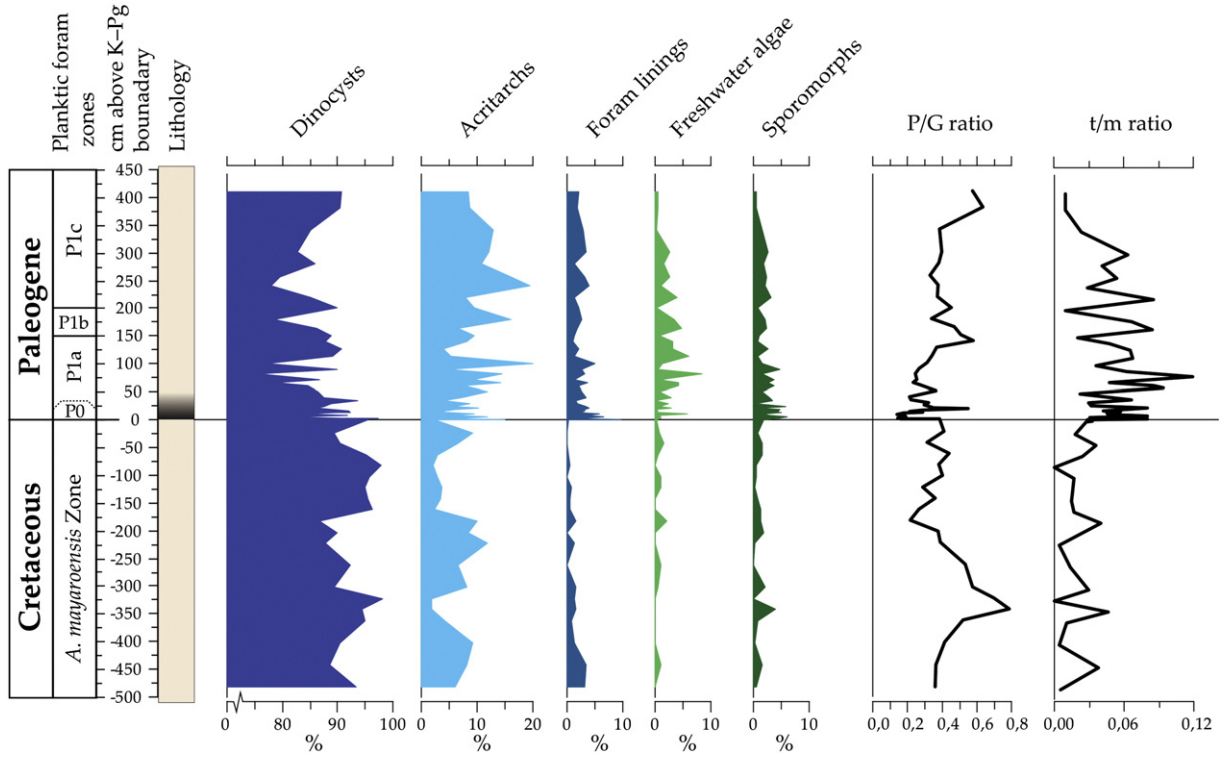

Fig. 5. The relative distribution of the recorded categories of palynomorphs, the P/G ratio sensu Versteegh (1994) and the ratio of terrestrial over marine palynomorphs (t/m ratio).

The result of the DCA analysis of the Elles section also has a resemblance to that of Brinkhuis et al. (1998). Although the position of species in the DCA-plot of the Elles section dataset is quite similar to the position of species in the El Kef section DCA, there are also some striking differences between these DCA-plots. One of these is that in the DCA of Brinkhuis et al. (1998) the first axis is determined by two main outliers, the A–P complex and *Areoligera senoniensis*, whereas in the Elles record, these taxa plot on different places in the DCA analysis. In our

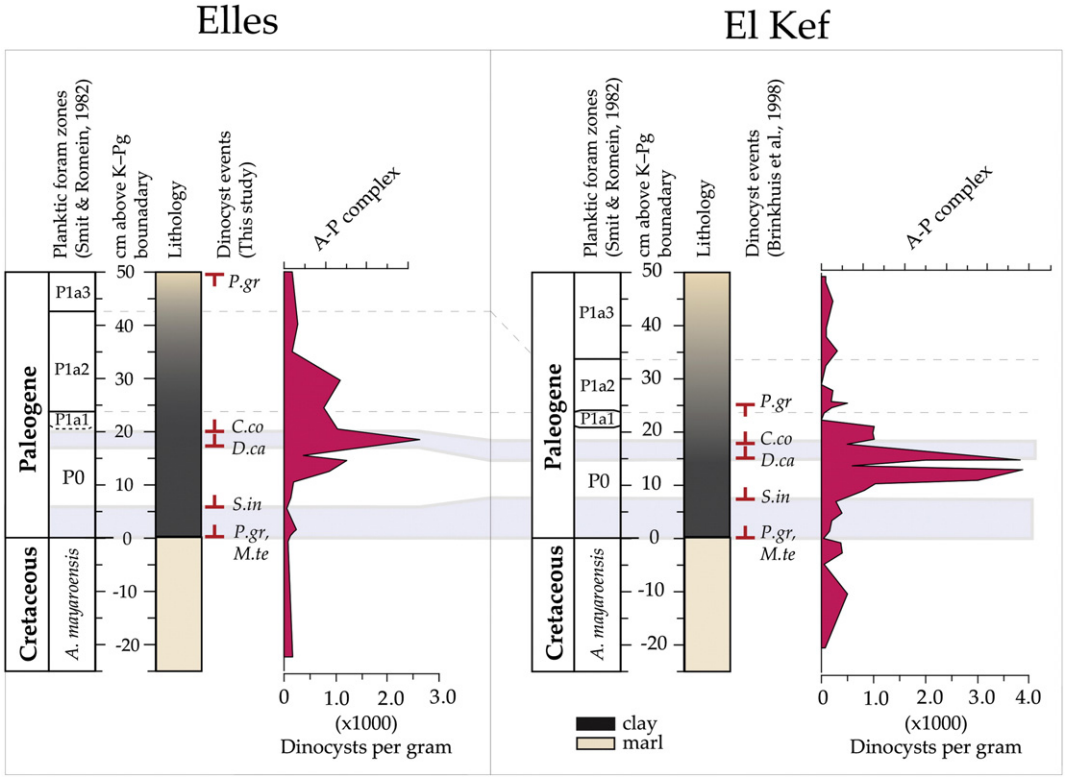

Fig. 6. The absolute abundances of the *Andalusiella–Palaeocystodinium* complex (A–P complex) in cysts per gramme at the boundary intervals of the Elles section and the El Kef section. Data of the El Kef section are from Brinkhuis et al. (1998), the data from the Elles section are from this study.

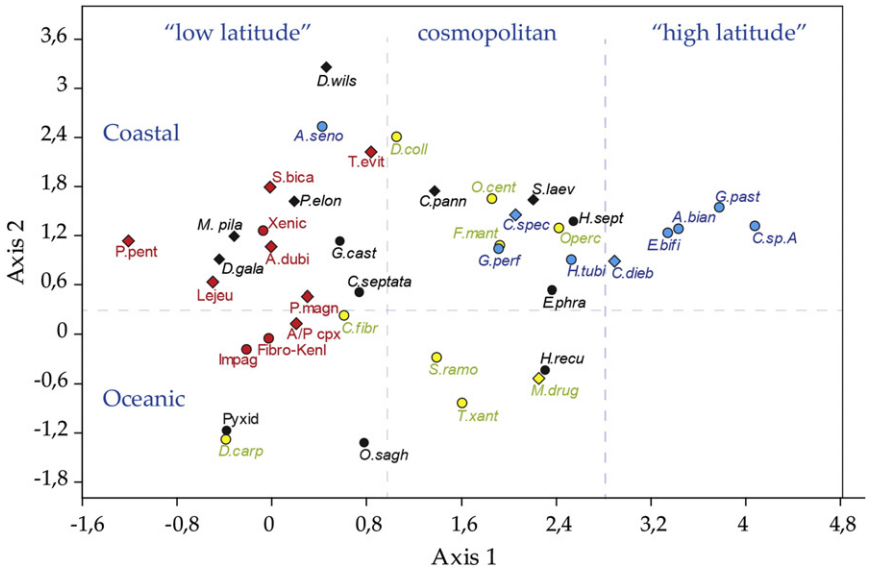

Fig. 7. Results of the Detrended Correspondence Analysis (DCA) of the Elles section dataset. (*A.bian* = *A. biannii*; *A.dubi* = *A. dubia*; A–P cpx = Andalusiella–Palaeocystodinium complex; *A.seno* = *A. senoniensis*; *C.dieb* = *C. diebelii*; *C.fibr* = *C. fibrospinosum*; *C.pann* = *C. pannunceum*; *C.sept* = *C. septata*; *C.sp.A* = *C.* sp. A; *C.spec* = *C. speciosum*; *D.carp* = *D. carposphaeropsis*; *D.coll* = *D. colligerum*; *D.gale* = *D. galeata*; *D.wils* = *D. wilsonii*; *E.bifi* = *E. bifidum*; *E.phra* = *E. phragmites*; Fibro/Kenl = Fibrocysta/Kenleya spp.; *F.mant* = *F. mantellii*; *G.cast* = *G. castelcasiensis*; *G.past* = *G. pastielsii*; *G.perf* = *G. perforata*; *H.recu* = *H. recurvatum*; *H.sept* = *H. septata*; *H.tubi* = *H. tubiferum*; Impag = *Impagidinium* spp.; Lejeu = *Lejeunecysta* spp.; *M.drug* = *M. druggii*; *M.pila* = *M. pilatum*; *O.cent* = *O. centrocarpum*; *O.isra* = *O. israelianum*; *O.sagh* = *O. saghirum*; *P.magn* = *P. magnificum*; Pyxid = *Pyxidinopsis* spp.; *P.elon* = *P. elongatum*; *S.bica* = *S. bicavatum*; *S.laev* = *S. laevigatum*; *S.ramo* = *S. ramosus*; *T.evit* = *T. evittii*; *T.xant* = *T. xanthiopyxides*; *P.pent* = *P. pentagonia*; Xenic = *Xenicodinium* spp.). The average latitudinal preference based on the literature review of Brinkhuis et al. (1998) are indicated, with low latitude taxa indicated in red, high-latitude taxa in blue and cosmopolitan taxa in yellow. Taxa with unknown latitudinal preferences are indicated in black. In the figure Gonyaulacoid dinocysts are indicated by circles, Peridinioid dinocysts are indicated by diamonds.

analysis of Elles, both plot within the cluster on the left-hand side and consequently, a different DCA axis is dominant. Also, several species that have been inferred to be high latitude taxa based on the literature review by Brinkhuis et al. (1998) do not show such a distribution in the DCA-analysis of the Elles section dataset, most notably *G. perforata* and *Cerodinium speciosum*. Since these taxa plot amongst cosmopolitan taxa such as *S. ramosus*, *Operculodinium centrocarpum* and *F. mantellii*, they possibly have a more cosmopolitan affinity. Of the taxa inferred to have a low-latitude affinity by Brinkhuis et al. (1998), most taxa show a similar distribution in the Elles dataset.

To test the robustness of the results of this DCA-analysis, we also performed a DCA analysis on the combined palynological countings of the El Kef and Elles sections (see Fig. 10). Similar to the DCA analysis on the El Kef dataset by Brinkhuis et al (1998), the first axis of this

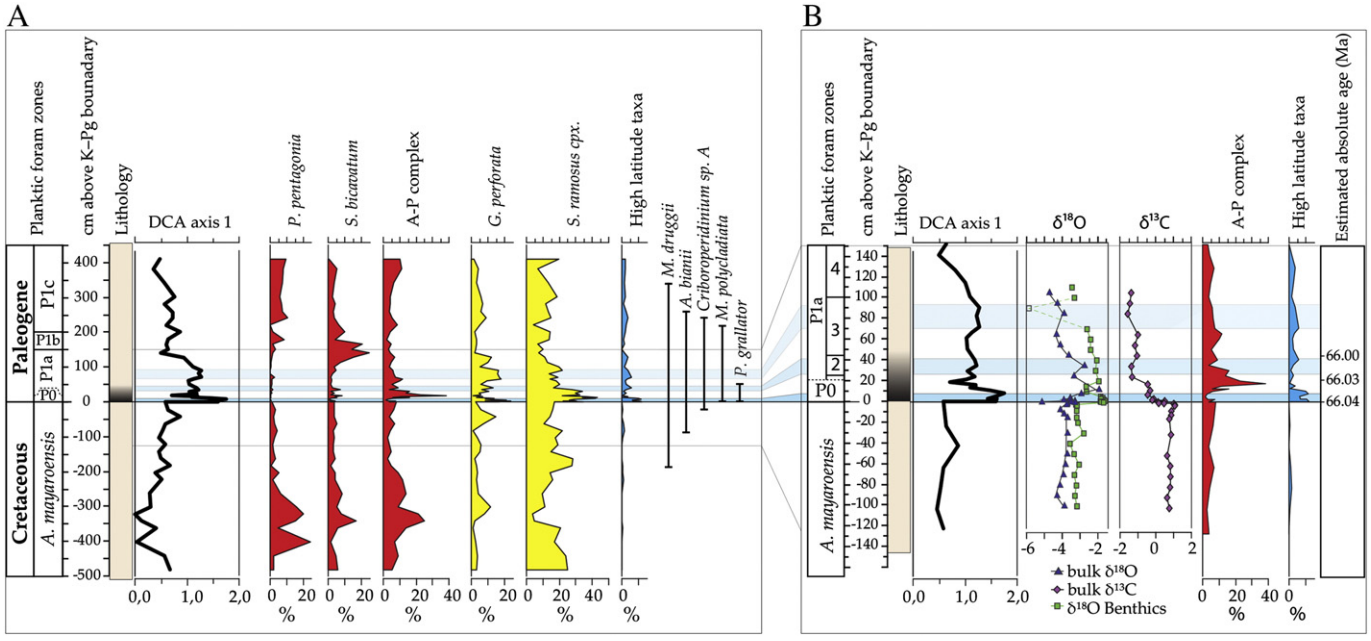

Fig. 8. Overview of various temperature indicators across the K–Pg boundary interval at Elles. A) The loadings on DCA-axis 1, relative abundances of 3 different inferred low-latitude taxa, 2 inferred cosmopolitan taxa and all inferred high-latitude taxa combined and the ranges of several inferred high-latitude taxa. B) A detail of the record across the K–Pg boundary, with the loadings on DCA-axis 1 and relative abundances of inferred high-latitude taxa of the Elles section compared with $\delta^{18}O$ of bulk carbonate and benthic foraminifera (*Anomalinoides acuta*) (Stüben et al., 2002) and bulk carbonate $\delta^{13}C$ of the parallel Elles II outcrop (Stüben et al., 2002). Estimated absolute ages are based on Arenillas et al. (2004) and Gradstein et al. (2012).

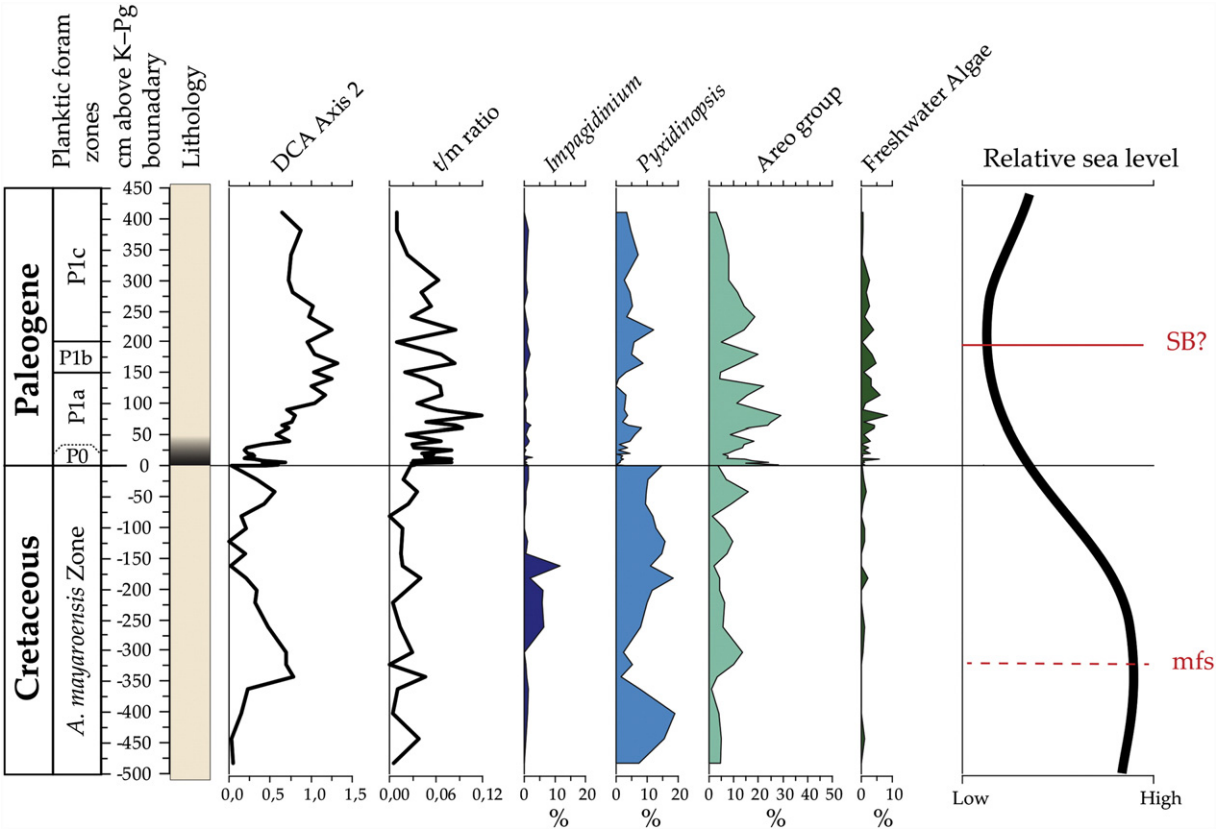

Fig. 9. Overview of different indicators of coastal proximity over the studied interval, with the loadings on DCA-axis 2 and the ratio of terrestrial palynomorphs over marine palynomorphs (t/m ratio). The relative abundances of the Impagidinium group (including all species of *Impagidinium* and *Pterodinium*) and Pyxidinopsis group (including all species belonging to *Pyxidinopsis* and *Xenicodinium*) are interpreted as indicators for offshore conditions (following Crouch and Brinkhuis, 2005) and relative abundances of the Areoligera group (including all species with dorsally-ventrally compressed (Gv) cysts, mainly *Glaphyrocysta* and *Areoligera*) and presumed fresh- and brackish water algae as indicators for inshore conditions (following Sluijs et al., 2005). The sequence stratigraphic interpretation of the palynological data is indicated on the right hand side.

DCA analysis (eigenvalue 0.2781) clusters most taxa relatively closely together, with the exception of *Areoligera senonensis* and *S. bicavatum*. The clustering is considered to represent relatively stable offshore, outer neritic conditions. *A. senonensis* and *S. bicavatum* only have elevated relative abundances in specific intervals and are considered to represent changes in environmental parameters, perturbing the stable offshore conditions (Brinkhuis et al., 1998). The second axis (eigenvalue 0.1094) appears to reflect a temperature signal, similar to DCA-axis 2 of the El Kef analyses and DCA-axis 1 of the Elles analyses, with most inferred higher-latitude taxa clustering at the bottom of the plot (see Fig. 10). Hence, this analysis shows that the signals within the palynological records of the El Haria formation K–Pg boundary interval are consistent and robust.

6. Discussion

6.1. Sea level trends

The loadings of the second axis of the DCA of the Elles section dataset show a minimum at about 150 cm below the boundary, at which point the oceanic genus *Impagidinium* also has its highest abundances. These results indicate that more oceanic conditions prevailed in the latest Maastrichtian, allowing the tentative placement of a maximum flooding surface (mfs). The record shows a sea level regression from 150 cm below the boundary upwards, with a sea-level lowstand between approximately 100 and 200 cm above the K–Pg boundary. Over this interval the *Areoligera*/*Glaphyrocysta* group, indicative of nearshore, shallow marine environments (Sluijs et al., 2005) becomes dominant and the ratio of terrestrial over marine palynomorphs increases. Similarly, freshwater algae and inferred freshwater tolerant dinocysts also have their highest abundance in this interval, suggesting it was characterized by the closest coastal proximity. This suggests that relative sea level was lowest in this interval, corresponding to a sequence boundary (SB). Several previous studies have suggested the presence of more than one SB in the interval above the K–Pg boundary, with sequence boundaries both at the base of Zone P1a as well as at the base of Zone P1b, which is compatible with the palynological record from the Elles section. In many shallower sections worldwide, this interval is marked by the presence of hiatuses (e.g., Macleod and Keller, 1991; Adatte et al., 2002; Schulte and Speijer, 2009). From this interval upwards, DCA-axis 2 decreases, the normal marine *Spiniferites* group becomes dominant again and the t/m ratio decreases. This could be interpreted as a gradual sea level rise continuing to the top of the section. These reconstructed sea level changes are consistent with the general trend that is recorded from sections worldwide (MacLeod and Keller, 1991; Habib et al., 1992; Moskovitz and Habib, 1993; Schulte and Speijer, 2009), which suggests that the recorded sea-level signals are global in nature. Hence, this global regression represents a background environmental change independent of the impact event, superimposed on which the impact-related perturbations occurred.

6.2. Climate change across the K–Pg boundary

In general, the dinocyst records of the Elles and El Kef sections are dominated by cosmopolitan and typical low-latitude species, such as the *S. ramosus* complex, *P. pentagonia* and *S. bicavatum*. This shows that the overall sea surface temperatures were likely relatively high in this region. At Elles, the upper Maastrichtian interval of 440 cm up to 220 cm below the K–Pg boundary is characterized by a dominance of these, and other typical low-latitude taxa, such as *Andalusiella polymorpha*

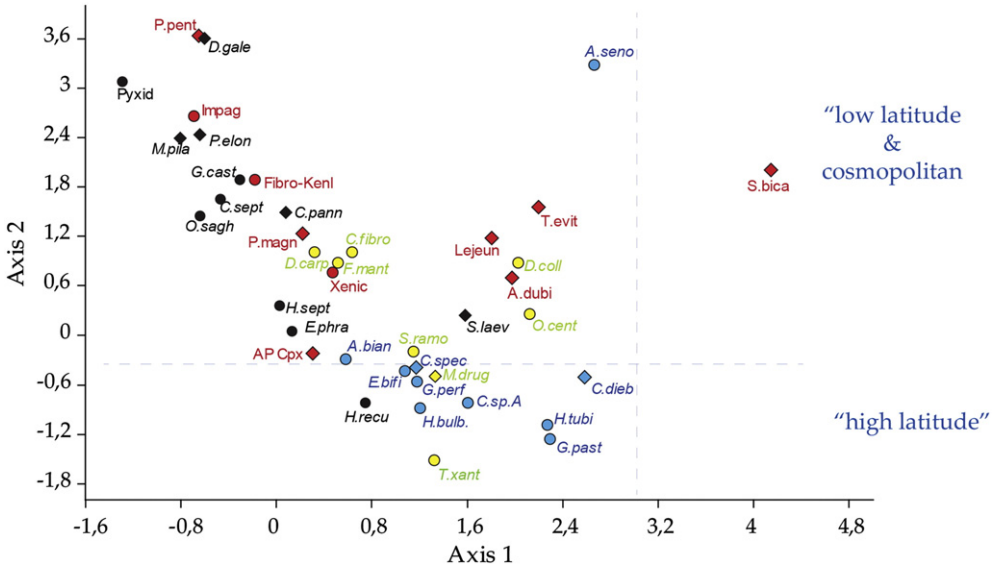

Fig. 10. Results of the Detrended Correspondence Analysis (DCA) of the combined datasets of the El Kef section (Brinkhuis et al., 1998) and the Elles section (this study). (*A.bian* = *A. biannii*; *A.dubi* = *A. dubia*; A–P cpx = Andalusiella–Palaeocystodinium complex; *A.seno* = *A. senoniensis*; *C.dieb* = *C. diebelii*; *C.fibr* = *C. fibrospinosum*; *C.pann* = *C. pannunceum*; *C.sept* = *C. septata*; *C.sp.A* = *C.* sp. A; *C.spec* = *C. speciosum*; *D.carp* = *D. carposphaeropsis*; *D.coll* = *D. colligerum*; *D.gale* = *D. galeata*; *E.bifi* = *E. bifidum*; *E.phra* = *E. phragmites*; Fibro/Kenl = Fibrocysta/Kenleya spp.; *F.mant* = *F. mantellii*; *G.cast* = *G. castelcasiensis*; *G.past* = *G. pastielsii*; *G.perf* = *G. perforata*; *H.bulb.* = *H.* bulbosum; *H.recu* = *H. recurvatum*; *H.sept* = *H. septata*; *H.tubi* = *H. tubiferum*; Impag = *Impagidinium* spp.; Lejeu = *Lejeunecysta* spp.; *M.drug* = *M. druggii*; *M.pila* = *M. pilatum; O.cent* = *O. centrocarpum*; *O.sagh* = *O. saghirum*; *P.magn* = *P. magnificum*; Pyxid = *Pyxidinopsis* spp.; *P.elon* = *P. elongatum*; *S.bica* = *S. bicavatum; S.laev* = *S. laevigatum*; *S.ramo* = *S. ramosus*; *T.evit* = *T. evittii*; *T.xant* = *T. xanthiopyxides*; *P.pent* = *P. pentagonia*; Xenic = *Xenicodinium* spp.). The average latitudinal preference based on the literature review of Brinkhuis et al. (1998) are indicated, with low latitude taxa indicated in red, high-latitude taxa in blue and cosmopolitan taxa in yellow. Taxa with unknown latitudinal preferences are indicated in black. In the figure Gonyaulacoid dinocysts are indicated by circles, Peridinioid dinocysts are indicated by diamonds.

and *Palaeocystodinium* cpx., resulting in high loadings on the first DCA-axis, revealing that this was likely the warmest interval. Above this, DCA-axis 1 reveals a general cooling trend up to the K–Pg boundary. Through this interval, inferred cosmopolitan species, such as the *S. ramosus* cpx, *G. perforata* and *F. mantelli*, become more dominant. In the upper 80 cm of the Maastrichtian, the first inferred cold water species, such as *Cribroperidinium* sp. A of Brinkhuis and Schiøler (1996) and *A. biannii*, make their appearance. The presence of *M. druggii* in this interval (see Fig. 8) might also be in agreement with this cooling. In the Maastrichtian, *Manumiella* is a typical southern hemisphere high-latitude genus (e.g., Elliot et al., 1994) and Habib and Saeedi (2007) suggested that the globally recorded *Manumiella* peak below the K–Pg boundary might be related to global cooling. Indeed, in the scatter plot of the DCA performed in the present study, this species plots close to other known high-latitude taxa. The ingression of typical higher-latitude dinocyst species in the uppermost Maastrichtian has also been recorded at several other sites (e.g., Habib et al., 1996), consistent with a cooling interval in the latest Cretaceous. This general cooling trend has also been inferred from uppermost Maastrichtian planktic foraminiferal oxygen isotope records (e.g., Olsson et al., 2002), plant macrofossil assemblages (Wilf et al., 2003) and faunal turnovers in for example planktic foraminifera (Abramovich and Keller, 2002) and calcareous nannofossil assemblages (Gardin, 2002). These studies suggested that the recorded cooling during the last 50–100 kyr of the Cretaceous actually reflects the aftermath of (i.e., the cooling that follows) a Late Cretaceous warming event, possibly related to Deccan Traps volcanism (Olsson et al., 2002).

At the K–Pg boundary, the dinocyst assemblage of the El Haria Formation changes dramatically. Our results confirm the rapid cooling pulse as recorded at the K–Pg boundary GSSP of El Kef. In the lowermost Danian (correlative to the base of Zone P0), several typical higher-latitude taxa make their first appearance and other inferred higher-latitude species become more dominant. Depending on the age model used, this first cooling pulse appears to have lasted between 1 and 5 kyrs (Galeotti et al., 2004; Gradstein et al., 2012). The P/G ratio indicates that marine productivity rapidly recovered within 5 cm above the boundary. The first presumably heterotrophic dinocysts that become dominant are taxa of the *Andalusiella–Palaeocystodinium* complex (A–P Cpx.). In the interval calibrated against the upper part of Planktic Foraminifer Zone P0 this complex of heterotrophic dinocyst shows a bloom, with up to 4000 cysts per gramme. Although the magnitude of this spike might be overestimated because sedimentation rates in the Danian are probably much lower than in the Maastrichtian as a consequence of the decreased input of $CaCO_3$ (Stüben et al., 2002), it most likely still represents an actual bloom, as it starts and ends within the boundary clay, the interval with lower sedimentation rates. This peak has been recorded at various sites in the Tethyan Ocean, for example in Tunisia and Spain (Brinkhuis et al., 1998), suggesting that this phenomenon is related to specific regional environmental conditions following the K–Pg boundary event. Eshet et al. (1994) identified high abundances of this A–P Cpx. as typical for a high productivity upwelling systems in the Tethyan Realm. Brinkhuis et al. (1998) describe this group as typical for high sea surface temperatures. This suggests that this group thrives in warm, relatively nutrient-rich settings. It is likely that the A–P Cpx is an opportunistic group that bloomed in the warm, nutrient rich conditions following the K–Pg boundary impact winter. Various other studies have recorded a variety of blooms of opportunistic groups occurring in the earliest Danian, taking advantage of access of nutrients and ecological space available (e.g., Gardin, 2002; Alegret and Thomas, 2009). This interval likely coincides with the episode of global warming following the K–Pg boundary, resulting from the release of greenhouse gases into the atmosphere (Kring, 2007; Vellekoop et al., 2014).

Subsequently, in the interval correlative to Zone P1a, the dinocyst record reveals less pronounced second and third cool water pulses (see Fig. 8). At both pulses there is an ingression of the inferred higher-latitude species, with every subsequent pulse appearing less pronounced than its predecessor, suggesting a kind of reverberation of the initial cooling pulse at the K–Pg boundary. Also at the El Kef stratotype section a multitude of cooling pulses was recorded (Brinkhuis et al., 1998; Galeotti and Coccioni, 2002; Galeotti et al., 2004), showing an overall

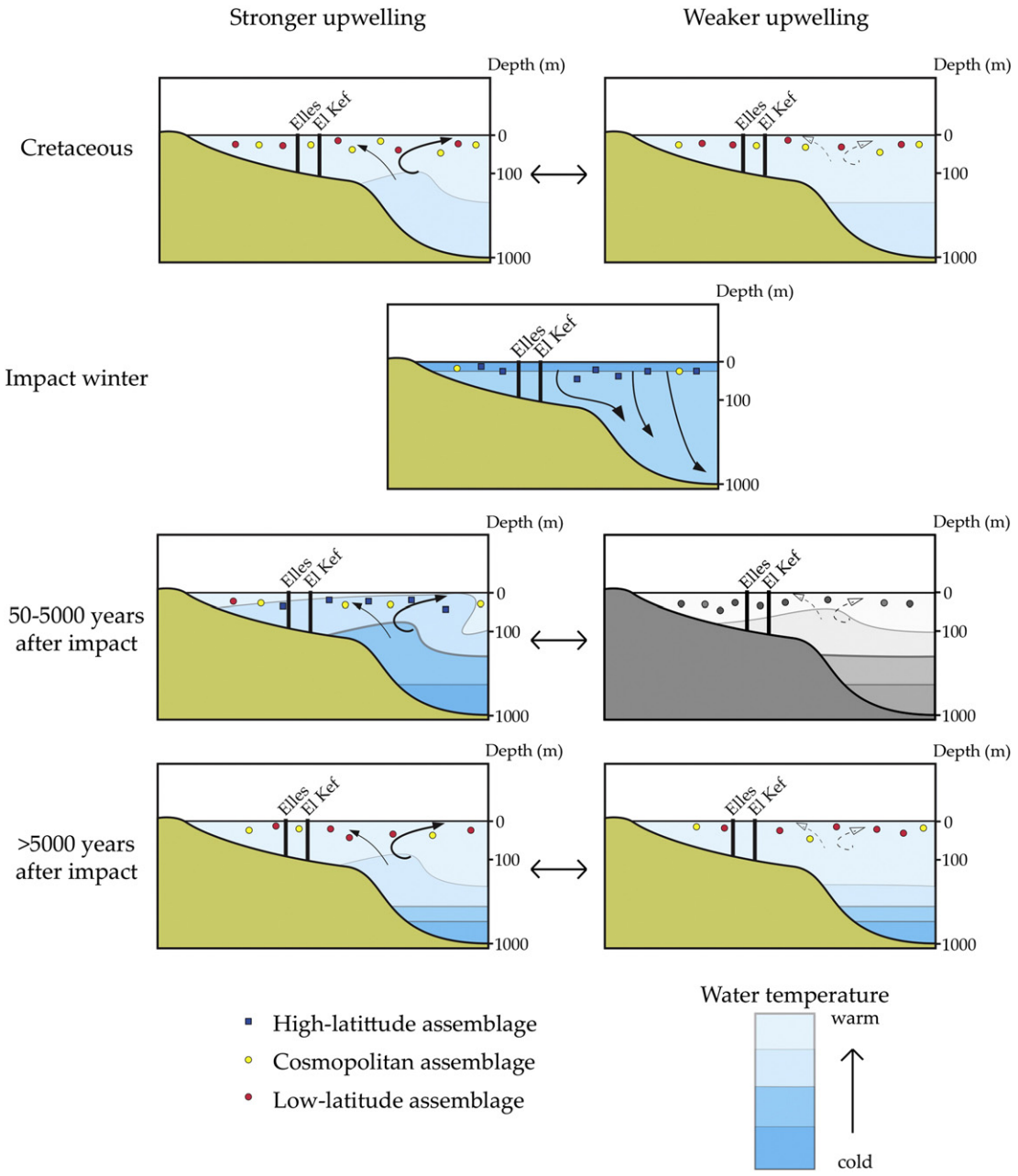

Fig. 11. Schematic illustration of the long term effects of an impact winter on a region influenced by upwelling. This situation along the Tunisian shelf is depicted for 4 different time intervals: late Maastrichtian; impact winter; the first thousands of years following the impact winter and >5000 years after the impact. For three of these time interval, the difference between stronger upwelling and weaker upwelling conditions is indicated and the consequences for the dinocyst assemblages.

similar pattern. The bulk $\delta^{18}O$ record of the parallel Elles II section shows positive shifts coinciding with these cooling pulses (Stüben et al., 2002; Fig. 8B). If these isotope shifts reflect an original, unaltered signal, they corroborate the cooling pulses recorded in the palynological record. Combined, these records suggest that the earliest Danian conditions were relatively unstable at the Tunisian continental shelf. Both at Elles and El Kef, this interval is also characterized by the ingressions of Boreal benthic foraminifera (Galeotti and Coccioni, 2002; Galeotti et al., 2004) and an increase in $\delta^{18}O$ values of benthic foraminifera (Stüben et al., 2002), suggesting that bottom and surface waters cooled simultaneously (see Fig. 8). Strikingly, while surface waters appear to be characterized by multiple cooling pulses, $\delta^{18}O$ values of benthic foraminifera suggest that the bottom waters remained cool over the entire interval. At approximately 100–120 cm above the boundary the benthic $\delta^{18}O$ values return to pre-impact values, above which point the dinocyst assemblage is again dominated by cosmopolitan and low latitude taxa and the bulk $\delta^{18}O$ has decreased to −5‰, slightly lower than pre-impact values. The low bulk $\delta^{18}O$ values and dominance of low latitude dinocyst taxa like *P. pentagonia*, *S. bicavatum* and *Thrithyrodinium evittii* shows that planktic foraminiferal (sub)zones P1a4 and P1b are characterized by relatively warm conditions. In the basal part of Zone P1c, cosmopolitan dinocyst species increase in abundance, suggesting that peak warmth had reduced by this time and the system stabilized again.

6.3. Potential cause for cooling pulses

The ingressions of higher-latitude taxa directly above the K–Pg boundary are likely a biological response to an 'impact winter' in the first years to decades following the Chixculub impact (Brinkhuis et al., 1998; Galeotti et al., 2004; Vellekoop et al., 2014). The cooling of sea surface waters is for example also recorded in the TEX_{86} sea surface temperature record from the Brazos River K–Pg boundary section

(Vellekoop et al., 2014). However, in Tunisia this phase appears to have lasted more than 10 kyrs (see Fig. 8), much longer than the months to decades predicted by numerical models and indicated by the TEX_{86} record from the Brazos River section (Vellekoop et al., 2014). In addition, the TEX_{86} record of Brazos River does not indicate any subsequent cooling pulses (Vellekoop et al., 2014). Both the prolonged duration of the cooling and its pulsating nature might be related to the presence of the North-Central Africa upwelling belt close to the studied sites (Parrish and Curtis, 1982; Huber and Sloan, 2001; Galeotti et al., 2004; Alsenz et al., 2013). A short impact winter, with a maximum duration of several decades, will have caused a rapid cooling of the global surface oceans, resulting in the formation of cold deep waters (Galeotti et al., 2004; see Fig. 11). When atmospheric and surface water temperatures rose again following the impact winter, this led to a temperature contrast between warm surface waters and cold, high-density deep waters and, hence, a sharpening and strengthening of the main thermocline. Because vertical mixing is limited under such conditions, the large volume of cold, high-density bottom waters will have persisted for time scales on the order of thousands of years (Galeotti et al., 2004), which is also evidenced by the $\delta^{18}O$ values of benthic foraminifera, indicating that bottom waters remained cool for thousands of years after the impact (Stüben et al., 2002; see Fig. 8). In an area influenced by upwelling, such as Tunisia, this would have resulted in the upwelling of cool waters, with a strong cooling effect on the surface waters, as evidenced by bulk $\delta^{18}O$ and dinocysts (see Fig. 8). In such a setting, minor, local variations in upwelling-intensity are likely to result in large fluctuations in surface water temperatures. The bulk $\delta^{13}C$ record of the Elles II section, presented by Stüben et al. (2002), shows slight shifts concurring with the cooling pulses, which might be related to small variations in upwelling-intensity (see Figs. 8 & 11). With time, the cold bottom waters will have slowly dissipated due to vertical mixing, decreasing their influence on the surface waters, which subsequently slowly returned to pre-impact conditions.

7. Conclusions

Our study provides an overview of the palynological record of the K–Pg boundary interval of the El Haria Formation. The dinocyst assemblages of the Elles section are almost identical compared to those of the El Kef K–Pg stratotype section. The El Haria assemblages are largely composed of species characteristic for an open marine shelf environment, and mainly includes typical cosmopolitan to warm water taxa. There is a clear sea-level signal in the dinocyst record, showing a general shallowing in the latest Cretaceous, reaching a sea level lowstand in the earliest Palaeocene. The dinocyst records of the El Haria Formation show several dinocyst events across the K–Pg boundary interval, likely indicating significant environmental perturbations. One of the most striking of these events is the ingression of higher-latitude dinocyst species in the first thousands of years after the impact, at both the El Kef and Elles sections. This ingression is likely related to a pronounced cooling resulting from a so-called global 'impact winter'. Clearly, in Tunisia, the earliest Palaeocene is characterized by a prolonged cooling phase with multiple cooling pulses, likely related to upwelling of the large volume of colder bottom waters that was produced during the global impact winter. These colder bottom waters dissipated over longer timescales. Following the first cooling interval is a peak of the *Andalusiella–Palaeocystodinium* 'complex', similar to other sites across the Tethys. This peak can likely be explained as a bloom of opportunistic low-latitude taxa immediately succeeding the K–Pg boundary global impact winter.

Acknowledgements

We thank N. Welters, J. van Tongeren and J. Ossebaar for analytical assistance. We thank the editor, Prof. Finn Surlyk and the two anonymous reviewers for their comments and suggestions. Funding for this research was provided by Utrecht University and the Netherlands Organization for Scientific Research (open competition grant ALWPJ/09047 to Brinkhuis and Sinninghe-Damsté).

Supplementary data

Supplementary data to this article can be found online at http://dx.doi.org/10.1016/j.palaeo.2015.03.021.

References

Abramovich, S., Keller, G., 2002. High stress late Maastrichtian paleoenvironment: inference from planktonic foraminifera in Tunisia. Palaeogeogr. Palaeoclimatol. Palaeoecol. 178, 145–164.

Açikalin, S., Vellekoop, J., Ocakoğlu, F., Yilmaz, I.Ö., Smit, J., Altiner, S.Ö., Goderis, S., Vonhof, H., Speijer, R.P., Woelders, L., Fornaciari, E., Brinkhuis, H., 2015. Geochemical and palaeontological characterization of a new K–Pg Boundary locality from the Northern branch of the Neo-Tethys: Mudurnu–Göynük Basin, NW Turkey. Cretac. Res. 52, 251–267.

Adatte, T., Keller, G., Stinnesbeck, W., 2002. Late Cretaceous to early Paleocene climate and sea-level fluctuations: the Tunisian record. Palaeogeogr. Palaeoclimatol. Palaeoecol. 178, 165–196.

Alegret, L., Thomas, E., 2009. Food supply to the seafloor in the Pacific Ocean after the Cretaceous/Paleogene boundary event. Mar. Micropaleontol. 73, 105–116.

Alsenz, H., Regnery, J., Ashckenazi-Polivoda, S., Meilijson, A., Ron-Yankovich, L., Abramovich, S., Illner, P., Almogi-Labin, A., Feinstein, S., Berner, Z., Püttmann, W., 2013. Sea surface temperature record of a Late Cretaceous tropical Southern Tethys upwelling system. Palaeogeogr. Palaeoclimatol. Palaeoecol. 392, 350–358.

Alvarez, L.W., Alvarez, W., Asaro, F., Michel, H.V., 1980. Extraterrestrial cause for the Cretaceous–Tertiary extinction. Science 208 (4448), 1095–1108.

Arenillas, I., Arz, J.A., Molina, E., 2004. A new high-resolution planktic foraminiferal zonation and subzonation for the lower Danian. Lethaia 37, 79–95.

Berggren, W.A., Kent, D.V., Swisher III, C.C., Aubry, M.P., 1995. A revised Cenozoic geochronology and chronostratigraphy. In: Berggren, W.A., et al. (Eds.), l Geochronology, Time and Global Stratigraphic Correlation. Society of Economic Geologist and Paleontologist, Special Publication, pp. 129–212.

Brinkhuis, H., Biffi, U., 1993. Dinoflagellate cyst stratigraphy of the Eocene/Oligocene transition in Central Italy. Mar. Micropaleontol. 22, 131–183.

Brinkhuis, H., Leereveld, H., 1988. Dinoflagellate cysts from the Cretaceous/Tertiary boundary sequence of El Kef, Northwest Tunisia. Rev. Palaeobot. Palynol. 56, 5–19.

Brinkhuis, H., Schiøler, P., 1996. Palynology of the Geulhemmerberg Cretaceous/Tertiary boundary section (Limburg, SE Netherlands). Geol. Mijnb. 75 (2–3), 193–213.

Brinkhuis, H., Zachariasse, W.J., 1988. Dinoflagellate cysts, sea level changes and planktonic foraminifers across the Cretaceous–Tertiary boundary at El Haria, northwest Tunisia. Mar. Micropaleontol. 13, 153–191.

Brinkhuis, H., Bujak, J.P., Smit, J., Versteegh, G.J.M., Visscher, H., 1998. Dinoflagellate-based sea surface temperature reconstructions across the Cretaceous–Tertiary boundary. Palaeogeogr. Palaeoclimatol. Palaeoecol. 141, 67–83.

Coccioni, R., Marsili, A., 2007. The response of benthic foraminifera to the K–Pg boundary biotic crisis at Elles (northwestern Tunisia). Palaeogeogr. Palaeoclimatol. Palaeoecol. 255, 157–180.

Crouch, E.M., Brinkhuis, H., 2005. Environmental change across the Paleocene–Eocene transition from eastern New Zealand: a marine palynological approach. Mar. Micropaleontol. 56 (3/4), 138–160.

D'Hondt, S., 2005. Consequences of the Cretaceous/Paleogene mass extinction for marine ecosystems. Annu. Rev. Ecol. Evol. Syst. 36, 295–317. http://dx.doi.org/10.1146/annurev.ecolsys.35.021103.105715.

Elliot, D.H., Askin, R.A., Kyte, F.T., Zinsmeister, W.J., 1994. Iridium and dinocysts at the Cretaceous–Tertiary boundary on Seymour Island, Antarctica: implications for the K–T event. Geology 22, 675–678. http://dx.doi.org/10.1130/0091-7613(1994)022<0675:IADATC>2.3.CO;2.

Eshet, Y., Almogi-Labin, A., Bein, A., 1994. Dinoflagellate cysts, paleoproductivity and upwelling systems: a Late Cretaceous example from Israel. Mar. Micropaleontol. 23, 231–240.

Fensome, R.A., Williams, G.L., 2004. The Lentin and Williams Index of Fossil Dinoflagellates 2004 Edition. American Association of Stratigraphic Palynologists Foundation Contr. Series.

Galeotti, S., Coccioni, R., 2002. Changes in coiling direction of Cibicides pseudoacutus (Nakkady) across the Cretaceous–Tertiary boundary of Tunisia: palaeoecological and biostratigraphic implications. Palaeogeogr. Palaeoclimatol. Palaeoecol. 178, 197–210.

Galeotti, S., Brinkhuis, H., Huber, M., 2004. Records of post-Cretaceous–Tertiary boundary millennial-scale cooling from the western Tethys: a smoking gun for the impact-winter hypothesis? Geology 32 (6), 529–532.

Galeotti, S., Lanci, L., Baffa, E., Balzelli, G., Bucci, C., Brinkhuis, H., Monechi, S., Peeters, J., Smit, J., Speijer, R.P., Sprovieri, M., 2005. Orbitally paced cycles from the lowermost Danian Elles section (Tunisia): implications for high-resolution chronostratigraphy across the Cretaceous/Tertiary boundary. EGU General Assembly, Vienna, April 24–29, 2005. Geophysical Research Abstracts Vol. 7.

Gardin, S., 2002. Late Maastrichtian to early Danian calcareous nannofossils at Elles (Northwest Tunisia). A tale of one million years across the K–T boundary. Palaeogeogr. Palaeoclimatol. Palaeoecol. 178, 211–231.

Gradstein, F.M., Ogg, J.G., Schmitz, M.D., Ogg, G.M., 2012. The Geologic Time Scale 2012. v. 1&2. Elsevier, Boston, USA. http://dx.doi.org/10.1016/B978-0-444-59425-9.00004-4 (1144 pp).

Habib, D., Saeedi, F., 2007. The *Manumiella seelandica* global spike: cooling during regression at the close of the Maastrichtian. Palaeogeogr. Palaeoclimatol. Palaeoecol. 255, 87–97.

Habib, D., Moshkovitz, S., Kramer, C., 1992. Dinoflagellate and calcareous nannofossil response to sea-level change in Cretaceous–Tertiary boundary sections. Geology 20, 165–168.

Habib, D., Olsson, R.K., Liu, C., Moshkovitz, 1996. High-resolution biostratigraphy of sea-level low, biotic extinction, and chaotic sedimentation at the Cretaceous–Tertiary boundary in Alabama, north of the Chicxulub crater. Geol. Soc. Am. Spec. Pap. 307, 243–252.

Hammer, Ø., Harper, D.A.T., Ryan, P.D., 2001. PAST: paleontological statistics software package for education and data analysis. Palaeontol. Electron. 4 (1), 9pp.

Hill, M.O., Gauch, H.G.J., 1980. Detrended correspondence analysis: an improved. Vegetatio 42, 47–58.

Huber, M., Sloan, L.C., 2001. Heat transport, deep waters, and thermalgradients: Coupled simulation of an Eocene "greenhouse" climate. Geophys. Res. Lett. 28, 3481–3484.

Huguet, C., Hopmans, E.C., Febo-Ayala, W., Thompson, D.H., Sinninghe Damsté, J.S., Schouten, S., 2006. An improved method to determine the absolute abundance of glycerol dibiphytanyl glycerol tetraether lipids. Org. Geochem. 37 (9), 1036–1041.

Hull, P.M., Norris, R.D., Bralower, T.J., Schueth, J.D., 2011. A role for chance in marine recovery from the end-Cretaceous extinction. Nat. Geosci. 4, 856–860. http://dx.doi.org/10.1038/NGEO1302.

Hultberg, S.U., Malmgren, B.A., 1987. Quantitative biostratigraphy based on Late Maastrichtian dinoflagellates and planktonic foraminifera from Southern Scandinavia. Cretac. Res. 8, 211–228.

Karoui-Yaakoub, N., Zaghbib-Turki, D., Keller, G., 2002. The Cretaceous–Tertiary (K–T) mass extinction in planktic foraminifera at Elles I and El Melah, Tunisia. Palaeogeogr. Palaeoclimatol. Palaeoecol. 178, 233–255.

Kring, D.A., 2007. The chicxulub impact event and its environmental consequences at the Cretaceous–Tertiary boundary. Palaeogeogr. Palaeoclimatol. Palaeoecol. 255 (1–2), 4–21.

Lengger, S.K., Kraaij, M., Tjallingii, R., Baas, M., Stuut, J.B., Hopmans, E.C., Sinninghe Damste, J.S., Schouten, S., 2013. Differential degradation of intact polar and core glycerol dialkyl glycerol tetraether lipids upon post-depositional oxidation. Org. Geochem. 65, 83–93.

MacLeod, N., Keller, G., 1991. Hiatus distributions and mass extinctions at the Cretaceous/Tertiary boundary. Geology 19, 487–501.

Molina, E., Alegret, L., Arenillas, I., Arz, J., 2006. The Global Boundary Stratotype Section and Point for the base of the Danian Stage (Paleocene, Paleogene, "Tertiary", Cenozoic) at El Kef, Tunisia—original definition and revision. Episodes 29 (4), 263–273.

Moskovitz, S., Habib, D., 1993. Calcareous nannofossil and dinoflagellate stratigraphy of the Cretaceous–Tertiary boundary, Alabama and Georgia. Micropaleontology 39 (2), 167–191.

Olsson, R.K., Hemleben, C., Berggren, W.A., Huber, B.T., Editors and Members of the Paleogene Planktonic Foraminifera Working Group, 1999. Atlas of Paleocene Planktonic Foraminifera. Smithson. Contrib. Paleobiol. 85, 255.

Olsson, R.K., Miller, K.G., Browning, J.V., Wright, J.D., Cramer, B.S., 2002. Sequence stratigraphy and sea-level change across the Cretaceous–Tertiary boundary on the New Jersey passive margin. In: Koeberl, C., MacLeod, K.G. (Eds.), Catastrophic Events and Mass Extinctions: Impacts and Beyond. 356. Geological Society of America Special Paper, Boulder, Colorado, pp. 97–108.

Parrish, J.T., Curtis, R., 1982. Atmospheric circulation, upwelling, and organic-rich rocks in the Mesozoic and Cenozoic eras. Palaeogeogr. Palaeoclimatol. Palaeoecol. 40, 31–66.

Pierazzo, E., Hahmann, A.N., Sloan, L.C., 2003. Chicxulub and climate: radiative perturbations of impact-produced S-bearing gases. Astrobiology 3, 99–118.

Pope, K.O., Baines, K.H., Ocampo, A.C., Ivanov, B.A., 1997. Energy, volatile production, and climate effects of the Chicxulub Cretaceous/Tertiary impact. J. Geophys. Res. 102 (E9), 21,645–21,664.

Schouten, S., Hopmans, E.C., Schefuß, E., Sinninghe Damsté, J.S., 2002. Distributional variations in marine crenarchaeotal membrane lipids: a new tool for reconstructing ancient sea water temperatures? Earth Planet. Sci. Lett. 204, 265–274.

Schouten, S., Huguet, C., Hopmans, E.C., Keinhuis, M., V., M., Sinninghe Damsté, J.S., 2007. Analytical methodology for TEX_{86} paleothermometry by high-performance liquid chromatography/atmospheric pressure chemical ionization-mass spectrometry. Anal. Chem. 79 (7), 2940–2944.

Schouten, S., Hopmans, E.C., Sinninghe Damsté, J.S., 2013. The organic geochemistry of glycerol dialkyl glycerol tetraether lipids: a review. Org. Geochem. 54, 19–61.

Schulte, P., Speijer, R.P., 2009. Late Maastrichtian–Early Paleocene sea level and climate changes in the Antioch Church Core (Alabama, Gulf of Mexico margin, USA): a multi-proxy approach. Geol. Acta 7 (1–2), 11–34.

Schulte, P., Alegret, L., Arenillas, I., Arz, J.A., Barton, P.J., Brown, P.R., Bralower, T.J., Christeson, G.L., Claeys, P., Cockell, C.S., Collins, G.S., Deutsch, A., Goldin, T.J., Goto, K., Grajales-Nishimura, J.M., Grieve, R.A.F., Gulick, S.P.S., Johnson, K.R., Kiessling, W., Koeberl, C., Kring, D.A., Macleod, K.G., Matsui, T., Melosh, J., Montanari, A., Morgan, J.V., Neal, C.R., Nichols, D.J., Norris, R.D., Pierazo, E., Ravizza, G., Rebolledo-Vieyra, M., Reimond, W.U., Robin, E., Salge, T., Speijer, R.P., Sweet, A.R., Urrutia-Fucugauchi, J., Vajda, V., Whalen, M.T., Willumsen, P.S., 2010. The chicxulub asteroid impact and mass extinction at the Cretaceous–Paleogene boundary. Science 327, 1214–1218.

Scotese, C.R., 2004. A continental drift flipbook. J. Geol. 112 (6), 729–741.

Scotese, C.R., Dreher, C., 2012. GlobalGeology. http://www.GlobalGeology.com.

Siggurdsson, H., D'Hondt, S., Carey, S., 1992. The impact of the Cretaceous/Tertiary bolide on evaportie terrane and generation of major sulfuric acid aerosol. Earth Planet. Sci. Lett. 109, 543–559.

Slimani, H., Louwye, S., Toufiq, A., 2010. Dinoflagellate cysts from the Cretaceous–Paleogene boundary at Ouled Haddou, southeastern Rif, Morocco: biostratigraphy, paleoenvironments and paleobiogeography. Palynology 34 (1), 90–124.

Sluijs, A., Brinkhuis, H., 2009. A dynamic climate and ecosystem state during the Paleocene–Eocene Thermal Maximum: inferences from dinoflagellate cyst assemblages on the New Jersey Shelf. Biogeosciences 6 (8), 1755–1781.

Sluijs, A., Pross, J., Brinkhuis, H., 2005. From greenhouse to icehouse; organic-walled dinoflagellate cysts as paleoenvironmental indicators in the Paleogene. Earth Sci. Rev. 68, 281–315.

Smit, J., Romein, A.J.T., 1985. A sequence of events across the Cretaceous–Tertiary boundary. Earth Planet. Sci. Lett. 74, 155–170.

Stüben, D., Kramar, U., Berner, Z., Stinnesbeck, W., Keller, G., Adatte, T., 2002. Trace elements, stable isotopes, and clay mineralogy of the Elles II K–T boundary section in Tunisia: indications for sea level fluctuations and primary productivity. Palaeogeogr. Palaeoclimatol. Palaeoecol. 178, 321–345.

Stüben, D., Kramar, U., Berner, Z.A., Meudt, M., Keller, G., Abramovich, S., Adatte, T., Hambach, U., Stinnesbeck, W., 2003. Late Maastrichtian paleoclimatic and paleoceanographic changes inferred from Sr/Ca ratio and stable isotopes. Palaeogeogr. Palaeoclimatol. Palaeoecol. 199, 107–127.

Vellekoop, J., Sluijs, A., Smit, J., Schouten, S., Weijers, J.W.H., Sinninghe Damsté, J.S., Brinkhuis, H., 2014. Rapid short-term cooling following the Chicxulub impact at the Cretaceous–Paleogene boundary. Proc. Natl. Acad. Sci. U. S. A. 111 (21), 7537–7541. http://dx.doi.org/10.1073/pnas.1319253111.

Versteegh, G.J.M., 1994. Recognition of cyclic and non-cyclic environmental changes in the Mediterranean Pliocene. Mar. Micropaleontol. 23, 141–171.

Versteegh, G.J.M., Zonneveld, K.A.F., 1994. Determination of (palaeo-)ecological preferences of dinoflagellates by applying Detrended and Canonical Correspondence analysis to Late Pliocene dinoflagellate cyst assemblages of the south Italian Singa section. Rev. Palaeobot. Palynol. 84, 181–199.

Weijers, J.W.H., Schouten, S., Spaargaren, O.C., Sinninghe Damsté, J.S., 2006. Occurrence and distribution of tetraether membrane lipids in soils: Implications for the use of the TEX_{86} proxy and the BIT index. Org. Geochem. 37, 1680–1693.

Wilf, P., Johnson, K.R., Huber, B.T., 2003. Correlated terrestrial and marine evidence for global climate changes before mass extinction at the Cretaceous–Paleogene boundary. Proc. Natl. Acad. Sci. U. S. A. 100 (2), 599–604.

Williams, G.L., Brinkhuis, H., Pearce, M.A., Fensome, R.A., Weegink, J.W., 2004. Southern Ocean and global dinoflagellate cyst events compared: index events for the Late Cretaceous–Neogene. In: Exon, N.F., Kennett, J.P., Malone, M.J. (Eds.), Proc. ODP, Sci. Results. 189, pp. 1–98. http://dx.doi.org/10.2973/odp.proc.sr.189.107.2004.